2019 American Control Conference (ACC)
Philadelphia, PA, USA, July 10-12, 2019

Optimal Control of Free Boundary of a Stefan Problem for Metallurgical Length Maintenance in Continuous Steel Casting

Zhelin Chen, Joseph Bentsman, *Member*, *IEEE*, and Brian G. Thomas,

***Abstract*—An optimal control approach for minimizing metallurgical length deviation during casting speed increase under constraints on the secondary cooling flow rates for continuous steel casting process is proposed. The process is described as a single-phase Stefan problem. The temperature and the shell growth are controlled by the steel surface heat flux generated by the cooling sprays. A cost function reflecting the error in tracking of a reference shell thickness is chosen, and the control objective is formulated as the minimization of this cost function under the spray rate constraints. Finding the control law satisfying this objective is formulated as a two-step procedure. First, an analytical setting for the cost function minimization is established through deriving the corresponding direct, adjoint, and sensitivity systems. Then, a computational procedure for solving this analytical setting, which finds the actual control law, is given. A numerical example presents the application of the method proposed. The results are then extended to a 2D model, with the corresponding numerical example provided.**

I. Introduction

The continuous steel casting process can be described by 1D single-phase Stefan problem partial differential equations (PDE) [1], [2] or a more detailed enthalpy formulation [3]. A set of simplified 1D models could be assembled into a 2D cross-section transient model of the 3D slab solidification process through spatial step interpolation [4]. A 2D model could then be used to estimate the distributed temperature profile within the strand in real-time employing only boundary measurements.

The optimal control of Stefan problem has been considered in several publications. In [5], the authors, first, proposed the optimal control law for a one-phase Stefan problem to maximize the interface movement in certain time through boundary input, and then proved the control law uniqueness. The problem considered in the present work is more complicated and optimal control to address it cannot be proposed beforehand. In [6], a bang-bang optimal periodic boundary control for a two-phase Stefan problem is derived to track a reference temperature distribution. However, the present work considers a different problem – control of the solid-liquid interface through flux input at the fixed boundary. In [7], a series representation of the solution of a one-dimensional one-phase Stefan problem is used to study motion planning through a boundary control. Hinze and Ziegenbalg [8] represent the interface in a two-phase Stefan problem as the graph of a function over a rectangular domain. They use the temperature at the boundary of the container as the control variable and aim to track the desired interface motion. However, Dirichlet boundary control is not implementable in continuous steel casting, since cooling is accomplished through boundary heat flux extraction corresponding to Neumann boundary condition. In [2], [9], Petrus et al. proposed entropy-based state and output feedback control laws for simultaneous control of the surface and internal temperatures, as well as the solidification front position through Dirichlet boundary measurements and Neumann boundary control at the solid boundary.

The present work puts an emphasis on the metallurgical length maintenance problem, while neglecting temperature control. This leads to a different control objective - that of minimizing the time and the size of the deviation of the metallurgical length from the desired value. In order to solve this problem, an open-loop minimum-time optimal control problem needs to be formulated under hard constraints on the metallurgical length deviation from the desired value. The problem has been heuristically addressed through simulation for sudden speed drop [10] and sudden speed increase [11]. However, no rigorous derivation in support of the heuristically found control law has been provided. The present work partially fills this gap, providing the state-unconstrained non-minimum-time optimal control law derivation for the minimization of the deviation of the metallurgical length from the desired value under hard spray rate constraints. The resulting control law, however, turns out to be a smoothed-out version of the best bang-bang control law found heuristically in [11].

The problem of minimizing the metallurgical length deviation is addressed in the present work as follows. First, it is recast into a problem of tracking a reference shell solidification front, where Neumann boundary condition is used as the heat flux control input. Then, an appropriate cost function is formualted, and the resulting optimization problem is solved in two steps: first, derivation of the corresponding direct, adjoint, and sensitivity systems for the cost function minimization under the input constraints is carried out, and, then, a numerical procedure is formulated for solving this analytical setting, which computes the actual control law. To the best of our knowledge, no heat-flux-driven optimization of this problem has been studied previously. This paper, therefore, presents the first control law that manipulates the heat flux at the fixed boundary to optimize the 1D evolution of the free boundary, and extends the method to a multi-slice

This work was supported by the Continuous Casting Center at Colorado School of Mines, and NSF Award CMMI 1300907.

Z. Chen (email: zchen61@illinois.edu) and J. Bentsman (phone: 217-244-1076; email: jbentsma@illinois.edu) are with the University of Illinois Urbana-Champaign, 1206 W Green St, Urbana, IL, 61801, USA.

B.G. Thomas (email: bgthomas@mines.edu) is with Colorado School of Mines, 1610 Illinois St, Golden, CO, 80401, USA.

model to provide a 2D dynamic free boundary optimization, required for the continuous steel casting process. The paper is organized as follows. In Section II a brief description of the single-slice optimization problem is given, and the analytical problem solution setting is derived. In Section III, the method is extended to an *N*-slice model. Section IV describes the numerical approach. Section V presents the simulation results. The proofs of formal statements are omitted due to space limitation and will be provided in a separate publication.

II. Single-slice Optimization Problem

A. *Single-phase Stefan problem*

The domain of a moving 1-D slice is divided into two separate sub-domains, corresponding to the solid and the liquid steel phases. The heat flux removed from the material at the solid surface is directly proportional to the controlled flow rate of the water spray applied at the solid surface. Therefore, the control input is represented by the unidirectional heat flux Neumann boundary condition at the solid boundary. Temperature evolves according to the usual linear parabolic heat diffusion equations in each sub-domain. The free solidification boundary moves according to the temperature gradient at the liquid/solid interface, subject to the conservation of energy. The latter imposes the temperature gradient discontinuity at the free boundary due to the latent heat involved in the phase change. The following assumption is made:

(A1) $T_0(x)$ is continuous, $T_0(x) \le T_f$, $x \in (0, s_0)$, and $T_0(x) = T_f$, $x \in (s_0, L)$,

(A1) is a simplifying, but practically justified assumption, as discussed in [1]. With (A1), the continuous casting process can be modeled using the following single-phase Stefan problem:

$$T_t(x,t) = aT_{xx}(x,t), x \in (0, s(t)), 0 < t < t_f, \tag{1}$$

$$T\left(s(t),t\right) = T_f,\ 0<t<t_f, \left(s(0) = s_0 > 0\right), \tag{2}$$

$$T_x\left(0,t\right) = u\left(t\right), 0 < t < t_f, \tag{3}$$

$$T\left(x,0\right) = T_o\left(x\right),\ 0<x<L, \tag{4}$$

$$\dot{s}(t) = bT_x(s(t),t), 0 < t < t_f, \tag{5}$$

where the material is solid for $x \in (0, s(t))$ and liquid for $x \in (s(t), L)$, L is the half-thickness of the slab, T_f is the melting temperature, $a = k / \rho c_p$ is the thermal diffusivity, $b = k / \rho L_f$, the properties: k (thermal conductivity), ρ (density), c_p (specific heat), and L_f (latent heat) can vary with temperature, but stay strictly positive [3] and are assumed to be positive constants in this paper, $u(t)$ is the boundary heat flux extracted from the strand surface, and t_f is the total time needed for the slice shown in Figure 1 to move from the meniscus to the end of a caster. In the equations above, subscripts x and t indicate partial derivatives.

In an actual caster, the feasible range of the cooling water flow rates is hard-constrained by the physical limitation of the spray cooling system, making the possible heat flux at the strand surface hard-constrained and piecewise continuous:

$$M_1 \le u(t) \le M_2,\ 0 < t < t_f,\ \text{ where } M_1, M_2 > 0 .$$

B. *Optimal control in finite time*

In [10], bang-bang control sequences to minimize metallurgical length (ML) deviation during a sudden speed drop were designed. The present paper considers the same problem as in [11]: minimizing the ML deviation during a sudden, *and more dangerous due to the possibility of the molten steel escape*, casting speed increase.

Denote *z*-axis as the casting direction, where $z = 0$ and z_{end} represent, respectively, the meniscus and the end of the caster. ML is determined by the shell thickness profile along the caster, $s(z)$; therefore, the goal of minimizing the ML deviation can be recast into minimizing the deviation of the shell thickness profile from the reference one, $\bar{s}(z)$. By taking the Lagrangian reference frame, the simulation domain of the equations (1)-(5) moves in the casting direction at casting speed, $v_c\left(t\right)$. Therefore, assuming the domain starts at the meniscus at time t=0, the reference $\bar{s}(z), 0 < z < z_{end}$ can be transferred to time domain, $\bar{s}(t), 0 < z < t_f$, by

$$z\left(t\right) = \int_0^t v_c\left(\tau\right) d\tau \ \ and \ \ z_{end} = \int_0^{t_f} v_c\left(\tau\right) d\tau. \tag{6}$$

Even if the reference shell thickness profile along the *z*-axis, $\bar{s}(z)$, stays the same, the corresponding reference in time, $\bar{s}(t)$, may be different for different casting speed profiles.

In the present work, the case of a sudden casting speed increase is considered: a slice starts at the meniscus at t=0, with casting speed v_{c1} , and at $t = t^*$, the casting speed increases to v_{c2} . Let $s_1(t)$ and $\bar{s}(t)$ denote, respectively, the shell thickness profiles of the slice and the reference. At the time of casting speed change, the slice resides at location

$$z^* = v_{c1} t^* . \tag{7}$$

For this slice, the total residence time in the caster is

$$t_{f1} = t^* + \frac{z_{end} - v_{c1} t^*}{v_{c2}}. \tag{8}$$

Notice that under the settings of the present work, the shell thickness profile, $\bar{s}\left(z\right)$, is that uniquely realized at the casting speed v_{c1}. Therefore, $s_1\left(t\right) = \bar{s}\left(t\right)$ for $t \in \left(0, t^*\right)$. Then, the minimization of the metallurgical length deviation can be reformulated as the minimization of the difference between $s\left(t\right)$ and $\bar{s}\left(t\right)$ for the remaining travel time of this slice in the caster.

Define a new time coordinate, t', by taking a time shift of t^* , i.e. $t' = t - t^*$. Then, $s_1\left(t'\right)$ and $\bar{s}\left(t'\right)$ are defined on $t' \in \left(-t^*, t_f\right)$, where $t_f = t_{f1} - t^*$. Further, $\left(0, t_f\right)$ is the residence time of the slice subject to the optimal control after the speed increase.

Now, introduce the functional:

$$J_u(s) = \int_0^{t_f} (s(t') - \bar{s}(t'))^2 \, dt', \tag{9}$$

and consider the following control set:

$$U_{ad} = \{u \in L_\infty[0,t_f], M_1 \le u(t') \le M_2\} . \quad (10)$$

For simplicity, denote $J_u(s)$ as $J(u)$. Then, the optimal control problem can be described as:

Problem (I). Find $u^o(t') \in U_{ad}$ such that

$$J(u^o) = \min_{u \in U_{ad}} J(u) .$$

For the ease of notation, in the remaining part of this paper, t is used in place of t'.

C. *Existence of optimal control*

The existence and uniqueness of solution for the above single-phase Stefan problem under bang-bang control have been proven [11]. In this work, the existence of optimal solutions for Problem (I) is proven.

Theorem 1: *There exists an optimal control* $u^* \in U_{ad}$ *that solves Problem (I).*

D. *Derivation of the optimality system*

In this section, the first-order necessary optimality condition is derived for the minimization problem using the Lagrange approach. The following Lagrange functional is used (the *dx* and *dt* have been omitted for brevity):

$$\begin{aligned} L(u,T,s,p,q,h) = \int_0^{t_f} (s-\overline{s})^2 - \int_0^{t_f}\int_{s(t)} (T_t - aT_{xx})p \\ - \int_0^{t_f} (T_x(0)-u)q - \int_0^{t_f} (\dot{s} - bT_x(s(t)))h. \end{aligned} \quad (11)$$

The functions $p(x,t)$, $q(t)$, and $h(t)$ denote the Lagrange multipliers associated with (1)-(5). The first order necessary optimality condition for the optimization problem now is given by:

$$\nabla L = 0 ,$$

and the adjoint equation system for our problem is defined through

$$L_T\tilde{T} = 0 \;\; and \;\; L_s\tilde{s} = 0 ,$$

for all feasible directions $\tilde{T}$ and $\tilde{s}$. L_T and L_s here denote the directional derivatives of L with respect to T and s, respectively.

The directional derivative of L with respect to T takes the form

$$L_T\tilde{T} = -\int_0^{t_f}\int_0^{s(t)} (\tilde{T}_t - a\tilde{T}_{xx})p - \int_0^{t_f} \tilde{T}_x(0)q + \int_0^{t_f} b\tilde{T}_x(s(t))h \; . \quad (12)$$

Integrating by parts with respect to time and space, sorting the terms corresponding to their domains of integration, and using $\tilde{T}(x,0) = 0$ (since $T(x,0) = T_0$ is required explicitly) yields the adjoint system for temperature of the form

$$p(x,t_f) = 0, x \in (0, s(t_f)) \;, \quad (13)$$

$$p_x(0,t) = 0, t \in (0,t_f) \;, \quad (14)$$

$$h(t) = -\frac{a}{b} p(s(t),t), t \in (0,t_f) \,, \quad (15)$$

$$q(t) = -ap(0,t), t \in (0,t_f) \,, \quad (16)$$

$$p_t(x,t) + ap_{xx}(x,t) = 0, x \in (0, s(t_f)), t \in (0,t_f) \,, \quad (17)$$

$$\dot{s}(t)p(s(t),t) = ap_x(s(t),t), t \in (0,t_f) \;. \quad (18)$$

Next, reassembling the Lagrange function by integration by parts (similarly to $L_T\tilde{T}$), and substituting the already known parts of the adjoint equation system obtained above yields

$$L = \int_0^{t_f} (s-\overline{s})^2 + \int_0^{s_0} \tilde{T}(0)p(0) + \int_0^{t_f} uq - \int_0^{t_f} \dot{s}h \, .$$

The directional derivative with respect to s is equal to

$$L_s\tilde{s} = \int_0^{t_f} 2(s-\overline{s})\tilde{s} - \int_0^{t_f} \dot{\tilde{s}}h \, .$$

Integration by parts yields

$$L_s\tilde{s} = \int_0^{t_f} 2(s-\overline{s}+\frac{1}{2}h_t)\tilde{s} + \tilde{s}(t_f)h(t_f) - \tilde{s}(0)h(0) \, .$$

Using $\tilde{s}(0) = 0$ (since $s(0) = \overline{s}(0)$) and $h(t_f) = 0$ (which follows from (13) and (15)), the adjoint system for solidification front is given by

$$s(t) - \overline{s}(t) + \frac{1}{2}h_t(t) = 0 \, . \quad (19)$$

Now, with the adjoint system (13)-(19), the only missing ingredient of the desired optimality system is $L_u\tilde{u}$. Differentiating (11) with respect to u yields

$$L_u\tilde{u} = \int_0^{t_f} \tilde{u}q \, . \quad (20)$$

Equation (20) is the first order necessary optimally condition when the control u is unconstrained. In our case, for $u \in U_{ad}$, the optimality condition is replaced by a variational inequality (Chapter 3 of [12]), which has the form:

$$L_u(v-u) = \int_0^{t_f} q(t)(v-u) \ge 0 \quad (21)$$

for all boundary functions v satisfying $M_1 \le v \le M_2$.

In summary, the optimality system of the optimal control Problem (I) in the absence of control and state constraints is given by:

- the forward system (1)-(5)
- the adjoint system (13)-(19)
- the gradient equation (21)

III. Multi-slice Optimization Problem

The above optimization problem considers only a single slice of steel in the caster, and the boundary flux u can be chosen to best suit that particular slice's reference shell thickness. In commercial casters, however, the spray region is usually subdivided into several aggregated spray zones, each linking a group of spray nozzles together. Therefore, any slice inside the spray zone will be subject to the same boundary flux. Each spray zone may have a different feasible region, U_{ad} , since M_1, M_2 can be different based on the caster settings. Therefore, the optimal control problem described in Section II is for one spray zone, rather than for the entire caster. The results are, therefore, extended next from a single-slice/single-spray-zone setting to a multi-slice/single-spray-zone one.

A. *Control problem formulation*

Let $s_0^i, T_0^i, z_i, \overline{s}_i, t_{fi}, i = 1,2,...,N,$ be the initial shell thickness, the initial temperature, location of the speed jump, the reference shell thickness, and the residence time, respectively. If $z_1 > z_2 > ... > z_N$, then $t_{f1} < t_{f2} < ... < t_{fN}$.

Define the cost function:

$$J_N(u) = \sum_1^N \int_0^{t_{fi}} (s_i(\tau) - \overline{s}_i(\tau))^2 d\tau \ , \qquad (22)$$

under the following control set:

$$U_N = \{u \in L_\infty[0, t_{fN}], M_1 \le u(t) \le M_2\} \ .$$

Problem (II). Find $u^*(t) \in U_N$ such that

$$J_N(u^*) = \min_{u \in U_N} J_N(u) \ .$$

Theorem 2: *There exists an optimal control $u^* \in U_N$ that solves Problem (II).*

B. *Derivation of the optimality system*

In this section, the optimality system for *N* slices is derived. The following Lagrange functional is used:

$$L = \sum_{i=1}^N \int_0^{t_{fi}} (s_i - \overline{s}_i)^2 - \sum_{i=1}^N \int_0^{t_{fi}} \int_{s_i(t)} (T_{it} - aT_{ixx}) p_i$$

$$- \sum_{i=1}^N \int_0^{t_{fi}} (T_{ix}(0) - u) q_i - \sum_{i=1}^N \int_0^{t_{fi}} (\dot{s}_i - bT_{ix}(s_i(t))) h_i.$$

The functions $p_i(x,t), q_i(t), h_i(t), i = 1, 2, ..., N$ denote the Lagrange multipliers associated with (1)-(5). The adjoint equation system for our problem is defined through

$$L_{T_i} \tilde{T}_i = 0 \ \ and \ \ L_{s_i} \tilde{s}_i = 0, i = 1, 2, ..., N \ .$$

Following the same procedure as in Section II.D yields the following adjoint system for each slice *i*:

$$p_i(x, t_{fi}) = 0, x \in (0, s_i(t_{fi})) \ , \qquad (23)$$

$$p_{ix}(0, t) = 0, t \in (0, t_{fi}) \ , \qquad (24)$$

$$h_i(t) = -\frac{a}{b} p_i(s_i(t), t), t \in (0, t_{fi}) \ , \qquad (25)$$

$$q_i(t) = -ap_i(0, t), t \in (0, t_{fi}) \ , \qquad (26)$$

$$p_{it}(x,t) + ap_{ixx}(x,t) = 0, (0, s_i(t_{fi})) \times (0, t_{fi}) \ , \qquad (27)$$

$$\dot{s}_i(t) p_i(s_i(t), t) = ap_{ix}(s_i(t), t), t \in (0, t_{fi}) \ , \qquad (28)$$

$$h_{it}(t) = -2(s_i(t) - \overline{s}_i(t)), t \in (0, t_{fi}) \ . \qquad (29)$$

The gradient for the control is given by

$$L_u \tilde{u} = \int_0^{t_{f1}} \sum_{i=1}^N q_i \tilde{u} + \sum_{i=1}^N \int_{t_{fi}}^{t_{fi+1}} \sum_{i+1}^N q_i \tilde{u} \ , \qquad (30)$$

yielding

$$J'(u) = \begin{cases} -\sum_{i=1}^N q_i, & 0 \le t < t_{f1}, \\ -\sum_{k=i}^N q_k, & t_{fi} \le t \le t_{fi+1}, \\ -q_N, & t_{fN-1} \le t \le t_{f_N}. \end{cases} \qquad (31)$$

Now, with the adjoint system, the procedure described in Section II.D can be used to solve the minimization problem.

IV. Numerical Approach

In this section, a numerical approach to solving the proposed optimization problems is illustrated. The procedure used combines the explicit finite difference with the variable space grid (VSG) [13]. The number of spatial intervals between the fixed boundary $x = 0$ and the moving boundary $x = s(t)$ was kept constant and equal to N_x, so that the moving boundary always lay on the N^{th} grid. The grid at the time instance *t* is defined by

$$x_{i,j} = i\Delta x_j, \Delta x_j = \frac{s(t_j)}{N_x}, 0 \le i \le N_x. \qquad (32)$$

For the time discretization,

$$\tau = \frac{t_f}{N_t}, t_j = j\tau, j = 0, ..., N_t \ ,$$

with $\hat{T}_{i,j}$ being the discrete temperature $\hat{T}_{i,j} \approx T(x_i(t_j), t_j)$, $\hat{s}_j$ being the discrete free boundary $\hat{s}_j \approx s(t_j)$, $\hat{p}_{i,j} \approx \hat{p}(x_i(t_j), t_j)$ being the discrete adjoint temperature, and $\hat{q}_j \approx \hat{q}_2(t_j), \hat{h}_j \approx \hat{h}(t_j)$ being the adjoint boundary conditions. The discrete versions of the other variables are also denoted with a hat. In the presence of pointwise control constraints U_{ad}, the gradient method is used (Algorithm 1).

Algorithm 1: Adjoint-Based Projected Gradient Method
Input: u^0
Output: $\hat{u}, \hat{T}, \hat{s}, \hat{p}, \hat{q}, \hat{h}$
1. Initialize: $i = 0$.
while $1 \le k \le k_{max}$ **do:**
2. Solve the forward problem (1)-(5) for $\hat{T}^k$, $\hat{s}^k$.
3. Solve the adjoint problem (13)-(19) for $\hat{p}^k, \hat{q}^k, \hat{h}^k$.
4. Construct the descent direction from (20): $v^k = -\hat{q}^k$.
5. Determine δ^k from: $\delta^k := \min_\delta J(P_{[M_1,M_2]}(u^k + \delta v^k))$.
6. Set $u^{k+1} = P_{[M_1,M_2]}(u^k + \delta^k v^k), k \to k+1$.

In order to ensure that the computed controls $\hat{u} \in U$, the projection $P_{[M_1,M_2]}(u)$ is introduced and defined as:

$$P_{[M_1,M_2]}(u) = \min\{M_2, \max\{M_1, u\}\} \ . \qquad (33)$$

Suitable stopping criteria for Algorithm 1 are

$$k_{\max} := \min\{k : \frac{\hat{J}^{k-1} - \hat{J}^k}{\hat{J}^0} \le \epsilon_J\} \text{, or}$$

$$k_{max} = \min\{k : | \hat{u}^{k+1} - \hat{u}^k | \le \epsilon_u\} \ .$$

1) Forward step k.

Following the same procedure as in [13], (1)-(5) can be recast into the following discretized version for $j = 0, 1, 2, ..., N_x - 1$:

$$\hat{T}_{0,j+1}^k = (1 - \frac{2a\tau}{\Delta x_j^2}) \hat{T}_{0,j}^k + \frac{2a\tau}{\Delta x_j^2} \hat{T}_{1,j}^k - \frac{2a\tau}{\Delta x_j} u_j^k \ , \qquad (34)$$

$$\hat{T}^k_{i,j+1} = \hat{T}^k_{i,j} + \frac{\tau}{2\Delta x_j}\frac{x_{i,j}\dot{\hat{s}}_j}{\hat{s}_j}(\hat{T}^k_{i+1,j} - \hat{T}^k_{i-1,j}) + \frac{a\tau}{\Delta x_j^2}(\hat{T}^k_{i+1,j} - 2\hat{T}^k_{i,j} + \hat{T}^k_{i-1,j}),\ 1 \le i \le N_x - 1, \tag{35}$$

$$\hat{T}^k_{N_x,j} = T_f, \tag{36}$$

$$\hat{s}^k_{j+1} = \hat{s}^k_j + \frac{b\tau}{2\Delta x_j}(3\hat{T}^k_{N_x,j} - 4\hat{T}^k_{N_x-1,j} + \hat{T}^k_{N_x-2,j}). \tag{37}$$

Then, the algorithm for the forward step can be described as follows:

Algorithm 2: Forward step k
1. Initialize at t=0: $\hat{s}^k_0 = s_0, \hat{T}^k_{i,0} = T_0(x_{i,j})$.
while $1 \le j \le N_t - 1$ **do:**
2. Compute the temperature $\hat{T}^k_{i,j}$ through (34)-(36).
3. Compute the free boundary $\hat{s}^k_{j+1}$ through (37).
4. Compute the new grid $x_{i,j+1}$ through (32).

2) Backward step k

The backward problem uses the same grid $x_{i,j}$ as that used in the forward problem. Similarly, the following discretized version of the adjoint system is derived:

$$\hat{h}^k_{j-1} = \hat{h}^k_j + 2\tau(\hat{s}^k_j - \overline{s}_j)\ , \tag{38}$$

$$\hat{p}^k_{N_x,j-1} = -\frac{b}{a}\hat{h}^k_{j-1}\ , \tag{39}$$

$$\hat{p}^k_{0,j-1} = (1 - \frac{2a\tau}{\Delta x_j^2})\hat{p}^k_{0,j} + \frac{2a\tau}{\Delta x_j^2}\hat{p}_{1,j}\ , \tag{40}$$

$$\hat{p}^k_{i,j-1} = \hat{p}^k_{i,j} - \frac{\tau}{2\Delta x_j}\frac{x_{i,j}\dot{\hat{s}}_j}{\hat{s}_j}(\hat{p}^k_{i+1,j} - \hat{p}^k_{i-1,j}) + \frac{a\tau}{\Delta x_j^2}(\hat{p}^k_{i+1,j} - 2\hat{p}^k_{i,j} + \hat{p}^k_{i-1,j}), 1 \le i \le N_x - 1. \tag{41}$$

Then, the algorithm for the backward step can be given by:

Algorithm 3: Backward step k
1. Initialize at t=t_f : $\hat{p}^k_{i,N_t} = 0, \hat{h}^k_{N_t} = 0$.
while $1 \le j \le N_t - 1$ **do:**
2. Set boundary conditions $\hat{p}^k_{N_x,j}$ and $\hat{p}^k_{N_x,j}$ by (38)-(40).
3. Compute $\hat{p}^k_{i,j}$ by (41).

3) Computation of the gradient

The choice of the descent direction v^k in step 4 of Algorithm 1 corresponds to the negative gradient, i.e., the direction of steepest descent.

4) Line minimization

Exact computation of the step size δ^k in step 5 of Algorithm 1 is too complicated. Instead, the backtracking line search algorithm with Armijo condition (Chapter 3 of [14]) is used to determine an approximation to δ^k .

V. Numerical Results

The following simulations use the parameters given in Table I. The simulation code based on VGS grid was verified against an analytical solution to the Stefan problem with Dirichlet boundary condition from [15]. The simulated zone length is $z_{end} = 1.75$ m, and the speed increase is from $v_{c1} = 1.5$ m/min to $v_{c2} = 1.75$ m/min. The control constraints are $M_1 = 0.5 \times 10^4\ K/s,\ M_2 = 4.0 \times 10^4\ K/s$.

The spatial grid contains 21 points, and the temporal grid contains 10001 grid points, i.e. $N_x = 20$, and $N_t = 10000$, $\tau = 6 \times 10^{-3}$ s. The stopping criteria are chosen as $\epsilon_J = 1 \times 10^{-8}$ m and $\epsilon_u = 1 \times 10^{-2}$ K/s.

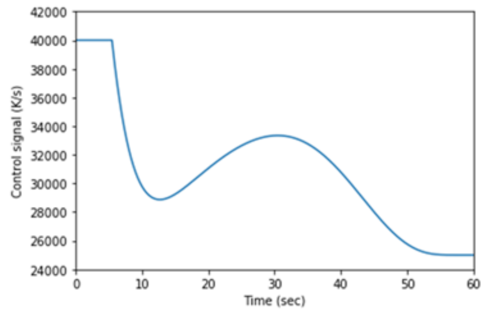

Figure 1. Optimal control signal for the single-slice optimization.

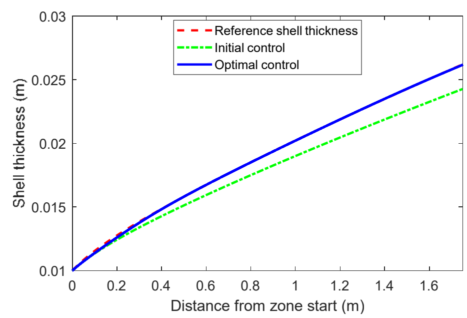

Figure 2. Shell thickness under initial control and optimal control.

A. *Single-slice optimization*

The initial shell thickness is $s_0 = 0.01$ m, the initial temperature T_0 is chosen to be linear with $T_0(s_0) = T_f$, $T_0(0) = 1473K$, the dwell time after speed increase is $t_f = z_{end} / v_{c2} = 60$ sec. The reference shell thickness is the one with casting speed v_{c1} and the initial control command $u(t) = 2.5 \times 10^4$ K/s.

After the speed increase, with the initial control $u(t)$, the cost value is $J(u) = 14.062$ mm^2; with the optimal control u^* shown in Figure 2, the cost goes down two orders of magnitude to $J(u^*) = 3.41 \times 10^{-2}$ mm^2. Figure 3 shows that the shell thickness under u^* matches the reference closely.

B. *Two-slice optimization*

Now, $N = 2$ is considered. At speed jump, the 1st slice is

TABLE I. THERMODYNAMIC PROPERTIES USED IN SIMULATIONS

Symbol	Description	Value
k	Thermal conductivity	30 W/mK
ρ	Density	7400 kg/m^3
c_p	Specific heat	670 J/kg
L_f	Latent heat of fusion	272 kJ/kg
T_f	Melting temperature	1811 K
L	Half thickness of strand	0.1 m

in the middle of the spray zone with $t_{f1} = 30$ sec, while the 2^{nd} slice is at the beginning of the spray zone with $t_{f2} = 60$ s. Therefore, the control $u(t)$ controls both slices for $0 \le t \le 30$ s, and controls only the 2^{nd} slice for $30 < t \le 60$ s.

With the initial control $u(t) = 2.5 \times 10^4$ K/s, $J(u) = 15.673$ mm^2; with the optimal control u^* shown in Figure 2, $J(u^*) = 0.42$ mm^2. Figure 4 shows the shell thickness profile along the casting direction z. The results show that the 2^{nd} slice has almost identical shell thickness as the reference, while the 1^{st} slice's shell thickness slightly differs from the reference.

The optimal control signal, shown in Figure 5, increases to maximum immediately after the speed increase to maximize the shell growth (this matches the finding in [10], [11]). The shape of the optimal control commands is similar to the three step bang-bang control found in [10], but more smoothed. The results also show that better control is attained over the 2^{nd} slice than the 1^{st} one. This difference takes place because at the moment of the speed increase, the 2^{nd} slice is at the beginning of the spray zone, allowing for more time to control its shell growth under input constraints.

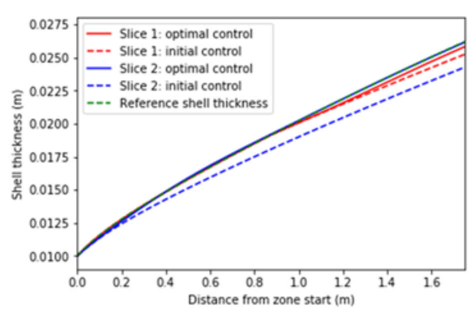

Figure 3. Shell thickness profile under initial control and optimal control for slice 1 and slice 2.

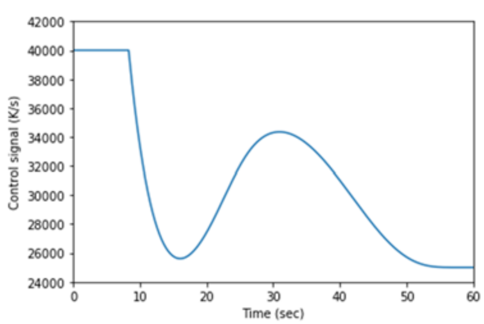

Figure 4. Optimal control signal for the two-slice optimization

VI. CONCLUSION

The problem of minimizing metallurgical length deviation during casting speed increase under heat flux constraints is formulated as tracking, under input constraints, of a predetermined free boundary profile. The single-slice model optimization approach is extended to the multi-slice model one. Numerical examples are presented, in which the tracking of the free boundary reference is attained. Future work will address multi-zone optimization.

Although the optimal control problem considered in this paper does not explicitly incorporate the minimum time requirement, the resulting control law turns out to be a smoothed-out version of the best minimum-time bang-bang control law found heuristically through simulation trial-and-error.

REFERENCES

[1] B. Petrus, Z. Chen, J. Bentsman, and B. G. Thomas, "Online Recalibration of the State Estimators for a System with Moving Boundaries Using Sparse Discrete-in-Time Temperature Measurements," *IEEE Trans. Automat. Contr.*, vol. 63, no. 4, pp. 1090–1096, 2018.

[2] B. Petrus, J. Bentsman, and B. G. Thomas, "Enthalpy-based Feedback Control Algorithms for the Stefan Problem," in *51st IEEE Conference on Decision and Control (CDC)*, 2012, pp. 7037–7042.

[3] Y. Meng and B. G. Thomas, "Heat Transfer and Solidification Model of Continuous Slab Casting: CON1D," *Metall. Mater. Trans. B*, vol. 34, no. 5, pp. 685–705, 2003.

[4] B. Petrus, K. Zheng, X. Zhou, B. G. Thomas, and J. Bentsman, "Real-Time, Model-Based Spray-Cooling Control System for Steel Continuous Casting," *Metall. Mater. Trans. B*, vol. 42, no. 1, pp. 87–103, 2011.

[5] A. Friedman and L.-S. JIANG, "Nonlinear Optimal Control Problems in Heat Conduction," *SIAM J. Control Optim.*, vol. 21, no. 6, pp. 940–952, 1983.

[6] A. Friedman, S. Huang, and J. Yong, "Optimal Periodic Control for the Two-Phase Stefan Problem," *SIAM J. Control Optim.*, vol. 26, no. 1, pp. 23–41, 1988.

[7] W. B. Dunbar, N. Petit, P. Rouchon, and P. Martin, "Motion planning for a nonlinear Stefan problem," *ESAIM Control. Optim. Calc. Var.*, vol. 9, pp. 275–296, 2003.

[8] M. Hinze and S. Ziegenbalg, "Optimal Control of the Free Boundary in A Two-Phase Stefan Problem," *J. Comput. Phys.*, vol. 223, no. 2, pp. 657–684, 2007.

[9] B. Petrus, J. Bentsman, and B. G. Thomas, "Application of Enthalpy-based Feedback Control Methodology to the Two-sided Stefan Problem," in *American Control Conference (ACC) 2*, 2014, pp. 1015–1020.

[10] Z. Chen, J. Bentsman, B. G. Thomas, and A. Matsui, "Study of spray cooling control to maintain metallurgical length during speed drop in steel continuous casting," *Iron Steel Technol.*, vol. 14, no. 10, pp. 92–103, 2017.

[11] Z. Chen, J. Bentsman, and B. G. Thomas, "Bang-Bang Free Boundary Control of a Stefan Problem for Metallurgical Length Maintenance," in *American Control Conference (ACC) 2018*, 2018, pp. 116–121.

[12] P. Neittaanmäki, D. Tiba, and J. Sprekels, *Optimization of Elliptic Systems: Theory and Applications,* Springer, 2006.

[13] J. Caldwell and Y. Y. Kwan, "Numerical Methods for One-Dimensional Stefan Problems," *Therm. Sci.*, vol. 13, no. 2, pp. 61–72, 2009.

[14] J. Nocedal and S. J. Wright, *Numerical Optimization*, 2nd ed., Springer, 2006.

[15] J. A. Dantzig and C. L. Tucker, *Modeling in Materials Processing*. Cambridge University Press, 2001.